Magnetic rotation and shape mixing in ^{134}Ce

S. Lakshmi,[1] H. C. Jain,[1] P. K. Joshi,[1] A. K. Jain,[2] and S. S. Malik[3]
[1]*Department of Nuclear and Atomic Physics, TIFR, Mumbai-400 005, India*
[2]*Department of Physics, IIT Roorkee, Roorkee, India*
[3]*Department of Physics, GND University, Amritsar-143 005, India*
(Received 22 August 2003; revised manuscript received 14 November 2003; published 30 January 2004)

High spin states of ^{134}Ce have been studied using an array of 8 Compton suppressed clover detectors and a multiplicity filter consisting of 14 NaI(T1) detectors. Two new $\Delta I=1$ bands $B4$ and $B5$ with strong intraband magnetic dipole transitions have been established. The crossover $E2$ transitions have been observed in the $B4$ band and lifetimes of levels, both in $B4$ and $B5$ bands, have been measured using the Doppler shift attenuation method. The measured $B(M1)$ values are large for the $B4$ band, yet the measured $B(M1)/B(E2)$ ratios are nearly constant with increasing frequency and do not support the magnetic rotation character. The $B4$ band also exhibits a small gain in alignment at a higher frequency suggesting an upbending and a band crossing. These features are sought to be explained in terms of two closely lying configurations $A:\pi(g_{7/2})^2\otimes\nu(h_{11/2}d_{3/2})$ and $B:\pi(h_{11/2})^2\otimes\nu(h_{11/2}d_{3/2})$, which have a small and a moderate deformation, respectively. The tilted axis cranking (TAC) calculations suggest that configuration B crosses the configuration A with a small alignment gain and mixing between the two may explain the observed features. The measured $B(M1)$ values deduced from the lifetimes for the $B5$ band show a decrease with increasing spin which is a characteristic feature of magnetic rotation bands. The results of the TAC calculations explain the $B5$ band very well by using the four-quasiparticle configuration $\pi(g_{7/2}h_{11/2})\otimes\nu(h_{11/2}^{-2})$ and establish it as a magnetic rotational band.

DOI: 10.1103/PhysRevC.69.014319 PACS number(s): 23.20.Lv, 21.10.Tg, 27.60.+j, 21.10.Ky

I. INTRODUCTION

Several rotationlike bands with strong $\Delta I=1$ transitions were observed in the early nineties in weakly deformed, neutron deficient Pb isotopes [1–3]. These were initially interpreted as oblate structures with high-K $h_{9/2}$ and $i_{13/2}$ protons coupled to the rotation aligned $i_{13/2}$ neutrons. However, the most striking feature of the bands, which is the existence of a long sequence of rotational transitions without considerable amount of deformation, remained a mystery. Later, an intuitively appealing idea, in terms of what is now known as the "shears mechanism," was proposed by Frauendorf [4,5] and these bands came to be known as magnetic rotation (MR) bands. In this picture, the valence high Ω proton particles (holes) and low Ω neutron holes (particles) or vice versa couple to form two long spin vectors j_π and j_ν, adding up to a total spin J of the nucleus. In the lowest energy state, the proton and neutron spin vectors are oriented almost perpendicular to each other resembling the blades of a shears. This coupling results in a large net transverse magnetic dipole moment which precesses around the total J and is responsible for the intense $M1$ radiation. The closing of the shears results in an increase of J and a decrease of the transverse magnetic dipole moment leading to a decrease in the $M1$ transition probabilities with increasing J. This is considered to be an important and most direct signature of the shears mechanism. Although the MR bands have been experimentally established in mass regions around $A\sim 190$, 110, and 80 [6–8] for sometime, the confirmed presence of such a band in mass 130 region has been reported in ^{136}Ce recently [9].

Nuclei in the mass 130 region exhibit several interesting features with the nucleons in $h_{11/2}$ orbitals driving the nucleus to nonspherical shapes. Although $\Delta I=1$ bands built on multi-quasiparticle structures have been observed earlier in this region [10–12] none of them were conclusively identified as MR bands. Recently, a $\Delta I=1$ band in ^{136}Ce has been interpreted as MR band by obtaining a direct confirmation of the decline in the $B(M1)$ values; a transition from the principal axis cranking to tilted axis cranking (TAC) induced by a shape change has also been witnessed for the first time [9] in this experiment. In the mass 130 region, the high-j bands involve low Ω protons and high Ω neutrons and provide a good testing ground for the shears mechanism. In the present paper, we focus our attention on the observation and interpretation of two new $\Delta I=1$ bands in ^{134}Ce. Our measurements confirm the existence of one $\Delta I=1$ magnetic rotation band similar to that observed in ^{136}Ce. The other $\Delta I=1$ band shows nearly constant $B(M1)/B(E2)$ ratios and $B(M1)$ values with increasing frequency. It has been interpreted as a tilted band arising from the mixture of two closely lying bands.

II. EXPERIMENT

The level structure of ^{134}Ce was earlier studied through (α, xn) reaction [13] and β decay of ^{134}Pr [14]. Highly deformed bands have also been reported by O'Brien *et al.* [15]. In the present work, the high spin states in ^{134}Ce have been studied through the ^{120}Sn(^{18}O, $4n$)^{134}Ce heavy-ion fusion evaporation reaction with a beam energy of 80 MeV. The experiment was carried out at the 14-UD pelletron accelerator in TIFR Mumbai, India, which delivered the 80 MeV ^{18}O beam on a 1.3 mg/cm^2 thick enriched ^{120}Sn target foil rolled onto a 15 mg/cm^2 thick Au backing. The γ decay following the reaction was studied using an array consisting of 8 Compton suppressed clover detectors with 14 NaI(T1)

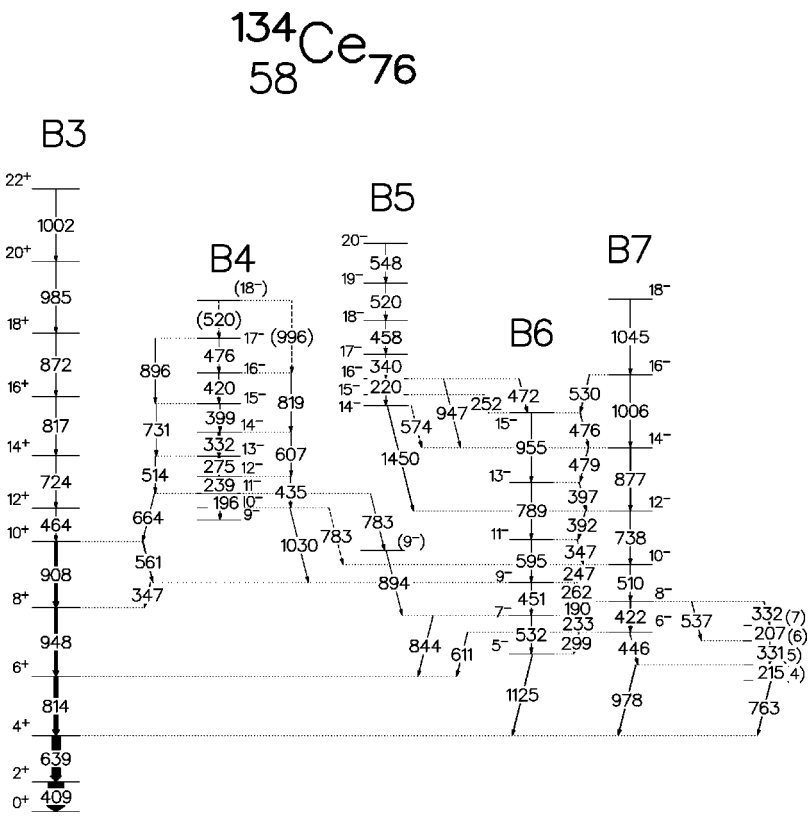

FIG. 1. Partial level scheme of ^{134}Ce.

multiplicity filter. This array was setup as a joint collaboration between TIFR, Mumbai, SINP and IUC-DAEF, Kolkata, and NSC, New Delhi [16,17]. The data were collected when three or more clovers fired along with two or more NaI(Tl) detectors. The decay scheme was established from the analysis of γ-γ coincidence data. The spins of levels and multipolarity of the γ transitions were obtained from the directional correlation orientation (DCO) ratios, angular distribution, and integrated polarization directional correlation measurements [18]. The DCO ratio is defined as

$$R_{\mathrm{DCO}} = \frac{\text{Intensity of } \gamma_1 \text{ observed at } 30\,^\circ \text{ and } 35\,^\circ \text{ gated on } \gamma_2 \text{ at } 75\,^\circ \text{ and } 90^\circ}{\text{Intensity of } \gamma_1 \text{ observed at } 75\,^\circ \text{ and } 90\,^\circ \text{ gated on } \gamma_2 \text{ at } 30\,^\circ \text{ and } 35^\circ}. \quad (1)$$

III. THE $\Delta I = 1$ BANDS

The partial level scheme of ^{134}Ce obtained from the present data is shown in Fig. 1. Several new transitions in ^{134}Ce have been observed in the present work. In particular, two bands with $\Delta I = 1$ transitions have been established for the first time. These bands are labeled as $B4$ and $B5$ in the level scheme. The transitions connecting the $B4$ band to the $B3$ band and those connecting the $B5$ band to the $B6$ band have been identified. The background subtracted gated spectra for the $B4$ band are shown in Fig. 2 and 3. The 239 +275 keV gated spectrum shows the presence of a sequence of low energy transitions shown in Fig. 2(a). The DCO ratio and the angular distribution measurements (see Table I) suggest $\Delta I = 1$ for the 196, 239, 275, 332, 399, 420, and 476 keV transitions. The measured polarization asymmetry established $M1$ multipolarity for the 239, 275, and 399 keV transitions. Other transitions in the cascade, i.e., 196, 332, 420, and 476 keV transitions, have been assumed to have $M1$ multipolarity. This assignment has been supported by the observation of the crossover $E2$ transitions shown in Figs. 2(b), 2(c), 3(a), and 3(b). The $M1$ multipolarities are also supported by the measured lifetimes and the $B(M1)$ values derived from them. The 664 and 783 keV transitions connecting the $B4$ band to the $B3$ and $B6$ bands, respectively, are also shown and labeled with an asterisk (*) in Fig. 3(a). The DCO ratio and polarization measurements (see Table I) suggest $\Delta I = 1$ and $E1$ multipolarity for the 664 keV transition, thereby fixing negative parity and $I = 11$ for the 4384 keV level in the $B4$ band. The γ gated spectra in Fig. 4(a) show transitions in band $B5$. The transitions connecting this band to the $B6$ and $B7$ bands are labeled with an asterisk (*) in

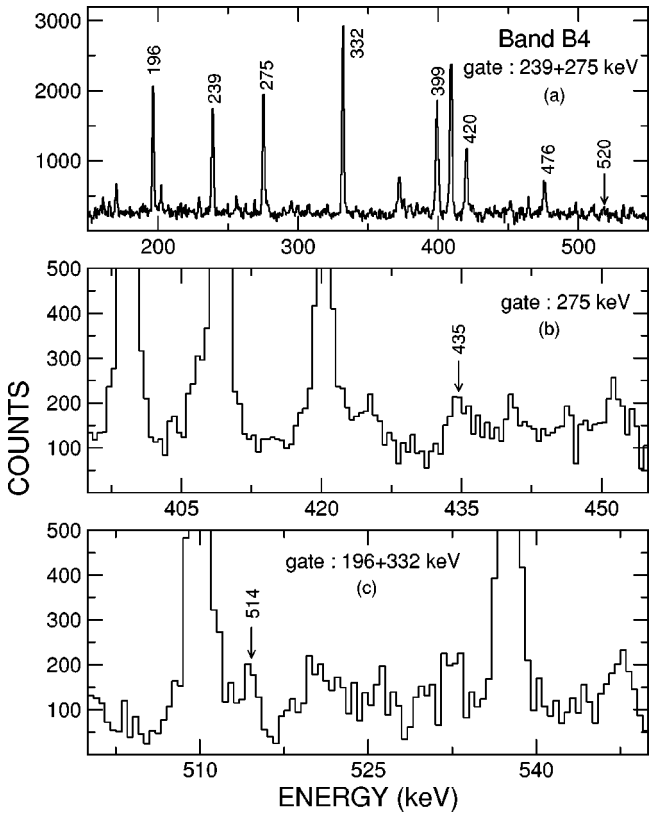

FIG. 2. (a) Background subtracted gated spectrum showing $M1$ transitions of band $B4$ in ^{134}Ce. (b),(c) Spectra showing the 435 and 514 keV crossover $E2$ transitions of band $B4$. The energies are labeled in keV.

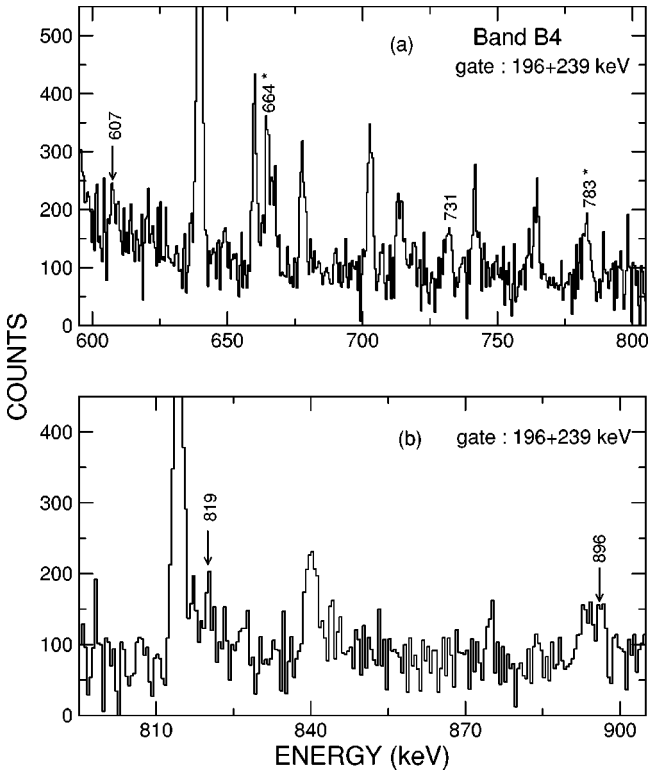

FIG. 3. (a),(b) Gated spectra showing the crossover $E2$ transitions and connecting transitions (labeled with an asterisk *) of band $B4$ in ^{134}Ce. The energies are labeled in keV.

TABLE I. Properties of transitions in $B4$ band and the connecting transitions observed in ^{134}Ce following the ^{120}Sn(^{80}O,$4n\gamma$) reaction.

E_γ (keV)	E_i (keV)	I_γ (%)	A_2/A_0	A_4/A_0	R_{DCO}	Polarization asymmetry	Multipolarity	Assignment
165.0	4188	0.23(4)					($M1$)	$10^- \rightarrow (9^-)$
196.2	4384	2.4(3)	−0.31(2)	0.39(3)	0.62(19)		$M1$	$11^- \rightarrow 10^-$
238.8	4623	3.8(3)	−0.45(3)	0.09(6)	0.44(9)	−0.06(3)	$M1$	$12^- \rightarrow 11^-$
275.3	4898	4.8(4)	−0.21(1)	−0.23(2)	0.48(10)	−0.05(4)	$M1$	$13^- \rightarrow 12^-$
331.7	5230	3.0(2)			0.64(9)		$M1$	$14^- \rightarrow 13^-$
398.8	5630	2.2(3)			0.50(18)	−0.09(4)	$M1$	$15^- \rightarrow 14^-$
408.9	409	100	+0.18(2)	−0.12(3)	0.97(7)	+0.06(1)	$E2$	$2^+ \rightarrow 0^+$
420.0	6050	2.4(2)			0.39(18)		$M1$	$16^- \rightarrow 15^-$
435.2	4623	0.23(7)					$E2$	$12^- \rightarrow 10^-$
475.5	6525	0.61(8)			0.47(16)		$M1$	$17^+ \rightarrow 16^+$
513.7	4898	0.49(4)					$E2$	$13^- \rightarrow 11^-$
607.2	5230	0.39(6)					$E2$	$14^- \rightarrow 12^-$
664.3	4384	2.8(3)			0.53(16)	+0.05(2)	$E1$	$11^- \rightarrow 10^+$
731.1	5630	0.44(4)					$E2$	$15^- \rightarrow 13^-$
783.1	4384	1.5(3)			1.57(94)		($E2$)	$11^- \rightarrow (9^-)$
819.1	6050	0.76(21)					$E2$	$16^- \rightarrow 14^-$
895.5	6525	0.16(2)					$E2$	$17^- \rightarrow 15^-$
1030.0	4188	< 0.2					$M1$	$10^- \rightarrow 9^-$

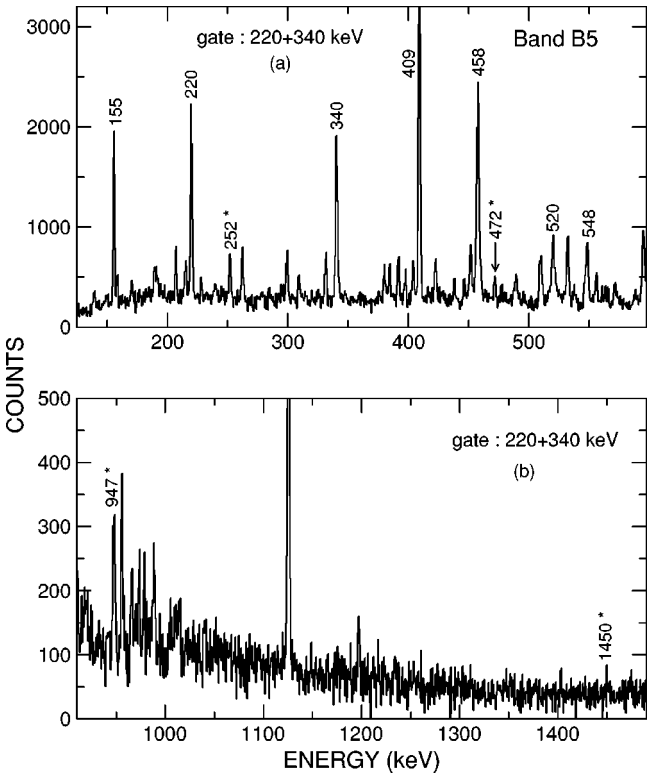

FIG. 4. (a),(b) Gated spectra showing the $M1$ transitions and connecting transitions (labeled with an asterisk *) of band $B5$ in ^{134}Ce. The energies are labeled in keV.

Figs. 4(a) and 4(b). The DCO ratio measurements suggest $\Delta I=1$ for transitions in the $B5$ band (see Table II). The measured polarization asymmetry shows $M1$ multipolarity for the 340 keV transition in the $B5$ band. Other transitions in the $B5$ band have been assumed to have $M1$ multipolarity. Although crossover $E2$ transitions are not observed in this band, but the measured lifetimes of four levels and the derived $B(M1)$ values support the assignment of $M1$ multipolarity to transitions in this band. The 472 keV connecting transition is also found to have $M1$ character with $\Delta I=1$ from the polarization measurements. Therefore, the 5969 keV level in the $B5$ band has been assigned $I=16$ and a negative parity since the $B6$ band has a negative parity (see Table III).

It is seen from Tables I and II that $M1$ transitions in both $B4$ and $B5$ bands have similar intensities. However, the crossover $E2$ transitions have been observed in the $B4$ band but not in band $B5$, thereby implying a stronger magnetic character or a relatively weaker deformation in the $B5$ band. The $B(M1)/B(E2)$ values deduced from the branching ratios for transitions in $B4$ band are listed in Table IV. These ratios exhibit a nearly constant behavior as a function of the rotational frequency $\hbar\omega$ as shown by filled circles in Fig. 5(c). The plots of the measured excitation energy vs $\hbar\omega$ and angular momentum I vs $\hbar\omega$ are shown in Fig. 5(a) and Fig. 5(b), respectively.

The $B(M1)$ values of the transitions in both the bands have been obtained through measurements of lifetimes using the Doppler shift attenuation method. Two-dimensional matrices were constructed with the detector at $\theta=30°, 60°, 120°$, or 145° along one axis and all other detectors along the other axis. The line shapes were projected for all angles with gates on stopped transitions below the transitions of interest. These experimental line shapes were fitted with the "LINESHAPE" analysis code of Wells and Johnson [19]. The slowing down history of the recoiling nuclei was generated using the Monte Carlo technique with 5000 histories and a time step of 0.001 ps. The electronic stopping powers of Northcliffe and Schilling [20] corrected for shell effects were used for calculating the energy loss. The side feeding was modeled to be transitions of independently variable lifetimes. The side feeding intensities were constrained to the experimental numbers. The topmost transition was fitted first and then the next lower one with top feeding taken from the fitted values of the transition above. Finally a global fit was obtained for the whole cascade with independently variable lifetimes for each level and their side feedings. The line shapes of 340, 458, 520, and 548 keV of the band $B5$ are shown in Fig. 6. Lifetimes extracted from these fits for the levels in band $B5$ are listed in Table V. The line shape fittings were obtained for the 420 and 476 keV transitions of band $B4$, and their lifetimes are listed in Table IV. The mea-

TABLE II. Properties of transitions in $B5$ band and the connecting transitions observed in ^{134}Ce following the ^{120}Sn(^{80}O,$4n\gamma$) reaction.

E_γ (keV)	E_i (keV)	I_γ (%)	A_2/A_0	A_4/A_0	R_{DCO}	Polarization asymmetry	Multipolarity	Assignment
155.5	5749	1.5(2)			0.62(23)		$M1$	$15^-\rightarrow14^-$
219.6	5969	4.3(4)	−0.32(2)	−0.33(2)	0.56(10)		$M1$	$16^-\rightarrow15^-$
251.7	5749	1.5(2)						$15^-\rightarrow15^-$
340.2	6310	6.4(4)			0.47(7)	−0.02(2)	$M1$	$17^-\rightarrow16^-$
457.6	6767	3.6(3)			0.58(15)		$M1$	$18^-\rightarrow17^-$
471.5	5969	1.3(1)			0.60(14)	−0.06(5)	$M1$	$16^-\rightarrow15^-$
519.8	7287	1.2(1)			0.60(22)		$M1$	$19^-\rightarrow18^-$
548.0	7835	1.0(1)			0.59(8)		$M1$	$20^-\rightarrow19^-$
947.4	5969	1.3(2)					$E2$	$16^-\rightarrow14^-$
1450.2	5594	<0.2				+0.17(8)	$E2$	$14^-\rightarrow12^-$

TABLE III. Properties of transitions in $B6$ and $B7$ bands and the connecting transitions observed in ^{134}Ce following the ^{120}Sn(^{80}O,$4n\gamma$) reaction.

E_γ (keV)	E_i (keV)	I_γ (%)	A_2/A_0	A_4/A_0	R_{DCO}	Polarization asymmetry	Multipolarity	Assignment
422.4	2896	13(1)			1.15(18)		$E2$	$8^-\rightarrow 6^-$
451.4	3158	12(1)			0.91(9)		$E2$	$9^-\rightarrow 7^-$
509.5	3405	12(1)			1.05(14)		$E2$	$10^-\rightarrow 8^-$
532.2	2706	14(1)			1.05(14)		$E2$	$7^-\rightarrow 5^-$
595.0	3753	11(1)			0.90(6)		$E2$	$11^-\rightarrow 9^-$
737.6	4143	11(1)	+0.20(3)	−0.26(5)	1.12(16)	+0.09(2)	$E2$	$12^-\rightarrow 10^-$
789.4	4542	11(1)			1.19(13)		$E2$	$13^-\rightarrow 11^-$
877.3	5020	6.9(5)			1.22(20)		$E2$	$14^-\rightarrow 12^-$
955.5	5497	4.4(4)			0.94(16)		$E2$	$15^-\rightarrow 13^-$
1006.0	6026	5.9(4)			1.46(43)		$E2$	$16^-\rightarrow 14^-$
1044.7	7070	2.0(2)			1.22(33)		$E2$	$18^-\rightarrow 16^-$
1125.2	2174	28(2)			0.57(08)	+0.04(1)	$E1$	$5^-\rightarrow 4^+$

sured spin vs rotational frequency $\hbar\omega$ for $B5$ band is plotted in Fig. 7(a) and the experimental $B(M1)$ values for 17^- to 20^- levels in this band are plotted in Fig. 7(b).

IV. RESULTS AND DISCUSSION

The observed characteristics of the two negative parity $\Delta I=1$ bands, i.e., $B4$ and $B5$ bands, have been compared with the results of the hybrid version of TAC calculations [21]. It is seen that the angular momentum of the band head and the level structure of $B5$ band closely resemble those of the $B3$ band in ^{136}Ce [9]. It suggests a similar four-quasiparticle configuration for the two bands. The observed similarity in the magnitude and behavior of $B(M1)$ values with increasing spin further strengthens the idea that the band $B5$ of ^{134}Ce is similar to band $B3$ of ^{136}Ce. We have, therefore, chosen a four-quasiparticle configuration $\pi(g_{7/2}h_{11/2})\otimes\nu(h_{11/2})^{-2}$ for the band $B5$ of ^{134}Ce. The pairing parameters were chosen as 80% of the odd-even mass difference, i.e., $\Delta_p=1.148$ and $\Delta_n=0.934$ MeV. The minimization of the total energy carried out in a self-consistent manner gave the deformation parameters $\epsilon_2=0.149$, $\epsilon_4=0.01$, $\gamma=43°$ and an average tilt angle $\theta\sim 35°$ for the angular momentum vector with respect to the principle axis x. The results of our calculations of spin vs rotational frequency $\hbar\omega$ show a very good agreement with the experimental values shown as filled circle in Fig. 7(a). Even the upbend at high frequencies is quite well reproduced. The calculated $B(M1)$ values shown in Fig. 7(b) also give a good agreement with the experimental data and strongly support the MR character of band $B5$.

The negative parity band $B4$ in ^{134}Ce exhibits several interesting features which require detailed calculations for its proper understanding. This band exhibits a mild backbending at $I=14\hbar$ with a gain in alignment of about $2\hbar$. The $B(M1)/B(E2)$ ratios show a nearly constant trend with increasing rotational frequency. However, the $B(M1)$ values, measured for two of the high spin transitions, are quite large, suggesting a magnetic character. We have carried out TAC calculations for all the possible four-quasiparticle configurations which lead to a negative parity band. On the basis of these calculations and the constraints of reproducing the observed band head spin and relative excitation energy of band $B4$ with respect to band $B5$ (band $B4$ is observed to lie lower than band $B5$), we have arrived at two possible configurations for the band $B4$: Configuration A: $\pi(g_{7/2})^2$

TABLE IV. Lifetimes, $B(M1)/B(E2)$, $B(M1)$, and $B(E2)$ values for transitions deexciting 12^- to 17^- levels of band $B4$ in ^{134}Ce. Errors on stopping power are not included.

E_γ (keV)	$I_i^\pi\rightarrow I_f^\pi$	$B(M1)/B(E2)$ $(\mu N/e\ \mathrm{b})^2$	τ (ps)[a]	$B(M1)$ (μ_N^2)	$B(E2)$ $(e\ \mathrm{b})^2$
239.0	$12^-\rightarrow 11^-$	13.0±3.9			
275.0	$13^-\rightarrow 12^-$	11.7±1.3			
332.0	$14^-\rightarrow 13^-$	12.1±2.1			
399.0	$15^-\rightarrow 14^-$	11.4±1.8		<0.75[b]	
420.0	$16^-\rightarrow 15^-$	11.0±3.1	$0.81^{+0.12}_{-0.12}$	$0.72^{+0.11}_{-0.11}$	$0.07^{+0.02}_{-0.02}$
476.0	$17^-\rightarrow 16^-$	13.8±2.4	$<0.82^{+0.10c}_{-0.10}$	$>0.51^{+0.06}_{-0.06}$	$>0.04^{+0.01}_{-0.01}$

[a]Lifetimes obtained from the weighted average of values at four angles $\theta=30°$, $60°$, $120°$, and $145°$.
[b]Assuming a lower limit of 1 ps for the mean lifetime of the level.
[c]Effective lifetime.

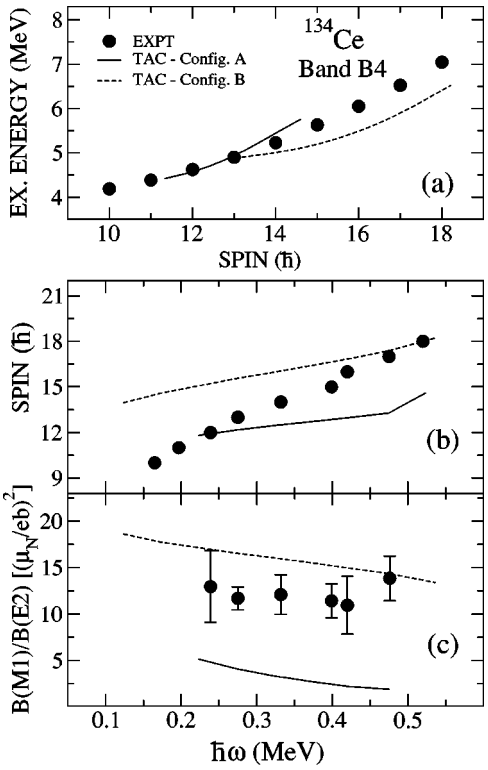

FIG. 5. (a) The experimental and calculated (TAC) excitation energies as a function of angular momentum for band $B4$ in ^{134}Ce. (b) The experimental and calculated angular momentum I vs frequency $\hbar\omega$. (c) The experimental $B(M1)/B(E2)$ values vs frequency $\hbar\omega$. The results of TAC calculations for the configuration A is shown as a solid line and the results for configuration B are shown as dotted line.

$\otimes \nu(h_{11/2}d_{3/2})$ and configuration B: $\pi(h_{11/2})^2 \otimes \nu(h_{11/2}d_{3/2})$.

The calculated deformation parameters for the configurations A and B are $\epsilon_2=0.016$, $\epsilon_4=0.015$, $\gamma=7°$ with an average tilt angle $\theta\sim 35°$ and $\epsilon_2=0.169$, $\epsilon_4=0.016$, $\gamma=28°$ with an average tilt angle $\theta\sim 65°$, respectively. The results of our calculations for the bands based on the configurations A and B are shown in Fig. 5. Both the bands are close to each other and lie lower than the $B5$ band. The calculated energies of the configurations A and B as a function of angular momentum are plotted in Fig. 5(a). It appears from this plot that the configuration B crosses the configuration A near $I=13\hbar$. The angular momentum I as a function of rotational frequency $\hbar\omega$ for both the configurations A and B along with the experimental data (filled circles) are plotted in Fig. 5(b). The gain in alignment in going from the configuration A to the configuration B is calculated to be of the order of $3\hbar$, whereas the observed gain in the alignment is of the order of $2\hbar$. A mixing of these two bands based on the configurations A and B may be able to explain the observed behavior of band $B4$. The $B(M1)/B(E2)$ ratios for the configuration A decrease marginally from 5 to 2 $(\mu_N/e\,\mathrm{b})^2$, whereas these values for the configuration B decrease from 17 to 13 $(\mu_N/e\,\mathrm{b})^2$ over the same rotational frequency range. The calculated $B(M1)/B(E2)$ ratios for both the configurations and also the experimental values are plotted in Fig. 5(c). The experimental values are found to lie between the calculated values for the two configurations being closer to configuration B, but do not show any significant decrease. The experimental and calculated $B(M1)$ values as a function of $\hbar\omega$ are also plotted in Fig. 8. Since the 399 keV transition did not show a line shape, the 15^- level in $B4$ band is assumed to have a lower limit of 1 ps for its lifetime. This leads to an upper limit of 0.75 $(\mu_N)^2$ for the $B(M1)$ value of the

TABLE V. Lifetimes and $B(M1)$ values for transitions deexciting 17^- to 20^- levels of band $B5$ in ^{134}Ce. Errors on stopping power are not included.

E_γ (keV)	$I_i^\pi \rightarrow I_f^\pi$	τ (ps)[a]	$B(M1)$ (μ_N^2)[b]
340.2	$17^- \rightarrow 16^-$	$0.85^{+0.07}_{-0.07}$	$1.71^{+0.13}_{-0.14}$
457.6	$18^- \rightarrow 17^-$	$0.34^{+0.03}_{-0.03}$	$1.76^{+0.17}_{-0.15}$
519.7	$19^- \rightarrow 18^-$	$0.28^{+0.03}_{-0.03}$	$1.47^{+0.16}_{-0.14}$
547.6	$20^- \rightarrow 19^-$	$<0.28^{+0.03c}_{-0.04}$	$>1.24^{+0.17}_{-0.14}$

[a]Lifetimes obtained from the weighted average of values at four angles $\theta=30°, 60°, 120°$, and 145°.
[b]Assuming pure $M1$ transitions since crossover $E2$ transitions have not been observed.
[c]Effective lifetime.

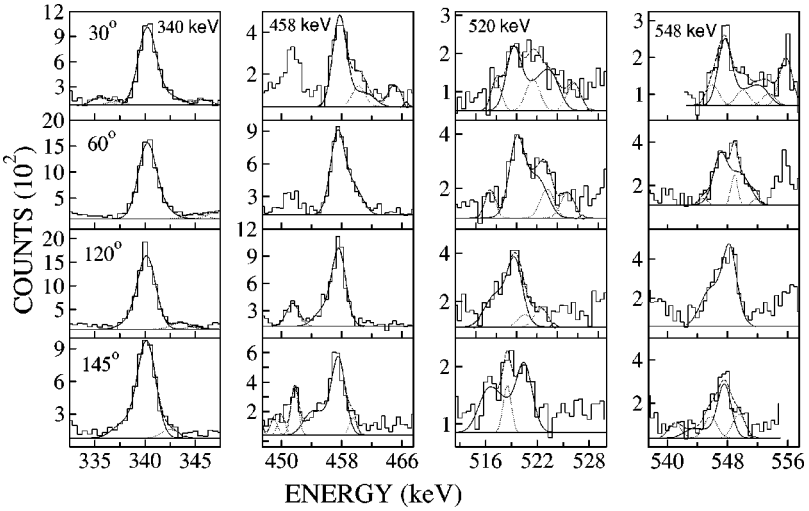

FIG. 6. Experimental and theoretical line shapes for the 340, 458, 520, and 548 keV γ rays at the forward $30°, 60°$, and backward $120°, 145°$ angles with respect to the beam direction in the $B5$ band of ^{134}Ce. The contaminant peaks are shown in dotted lines and line shapes for γ rays of interest are shown with solid lines.

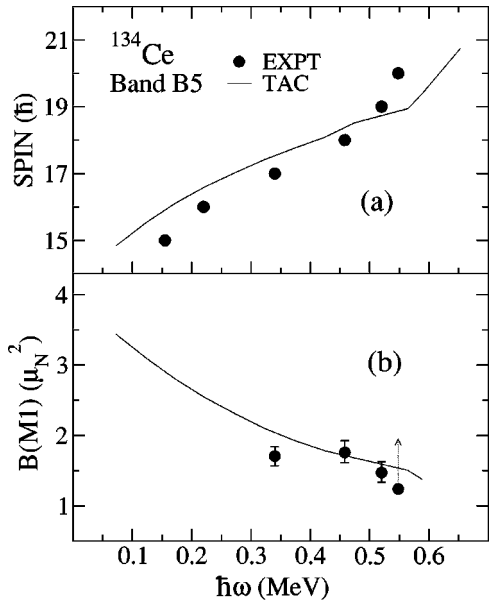

FIG. 7. (a) The experimental and calculated (TAC) angular momentum I vs frequency $\hbar\omega$ for the $B5$ band in ^{134}Ce. (b) The experimental $B(M1)$ values vs frequency $\hbar\omega$ for transitions in the $B5$ band in ^{134}Ce. The results of TAC calculations for the shape parameters $\epsilon_2=0.15$, $\gamma=43°$ and the tilt angle $\theta=35°$ are shown as solid line.

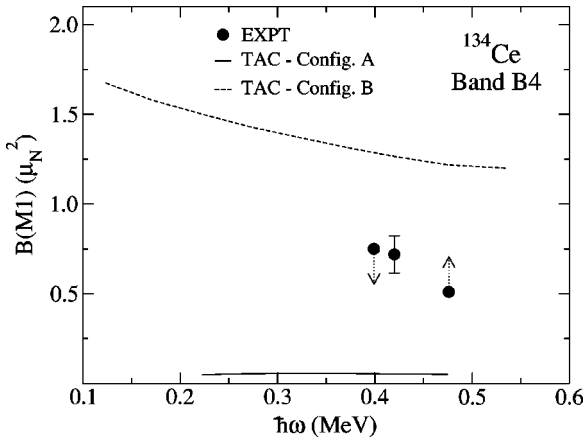

FIG. 8. The experimental $B(M1)$ values vs frequency $\hbar\omega$ for transitions in the $B4$ band in ^{134}Ce. The results of TAC calculations for the configuration A with shape parameters $\epsilon_2=0.016$, $\gamma=7°$ and the tilt angle $\theta\sim35°$ are shown with solid line and for configuration B with shape parameters $\epsilon_2=0.169$, $\gamma=28°$ and the tilt angle $\theta\sim65°$ are shown with dotted line.

399 keV transition, thereby indicating that the $B(M1)$ values may not be increasing appreciably with decreasing spin. TAC calculations predict large but decreasing $B(M1)$ with increasing spin for the configuration B but small and nearly constant values for the configuration A. Figure 8 shows that the experimental $B(M1)$ values also lie between the calculated values for the configurations A and B. It, therefore, appears that both the configurations may have a role to play in the $B4$ band. The behavior of the observed $B(M1)$ values along with the small gain in alignment suggest that band $B4$ could be a tilted band based on a small and a moderate deformation minimum lying close to each other. It may be noted that the principle axis cranking calculations carried out by us have been unable to explain the various features, and no such band has been observed by us in ^{136}Ce [9]. This indicates a sudden change in the structure due to decrease in neutron number by 2 in the mass 130 region.

V. CONCLUSIONS

In conclusion, two new $\Delta I=1$ bands $B4$ and $B5$ have been observed in ^{134}Ce for the first time. Both the bands appear to have four-quasiparticle configurations. The $B5$ band is strongly magnetic in character like the $B3$ band reported in ^{136}Ce [9]. The $B4$ band, on the other hand, shows experimental $B(M1)/B(E2)$ and $B(M1)$ values which lie between the theoretical values obtained for two different configurations A and B—the configuration B having larger $B(M1)$ values compared to the configuration A. It is proposed that the band $B4$ is a tilted band [22] with a mixing between the two closely lying minima corresponding to a small (prolate) and a moderate (triaxial) deformation. Nearly constant $B(M1)/B(E2)$ values do not support shears mechanism or magnetic rotation for this band.

ACKNOWLEDGMENTS

The clover array was setup at TIFR Pelletron jointly by TIFR, IUC-DAEF, Kolkata, SINP, Kolkata, and NSC, New Delhi. The authors would like to thank all participants of this joint national effort. Authors would also like to thank Dr. S. D. Paul, Dr. R. Palit, Dr. I. Mazumdar, and S. Nagaraj for their participation in data collection and the technical staff for smooth operation of the Pelletron. The partial support from the TIFR Endowment Fund, TIFR, Mumbai is acknowledged. Financial support from the Department of Science and Technology (Government of India) at Roorkee, and Department of Atomic Energy (Government of India) and Nuclear Science Center (UGC) at Amritsar is acknowledged.

[1] R. M. Clark *et al.*, Nucl. Phys. **A562**, 121 (1993).
[2] G. Baldsiefen *et al.*, Nucl. Phys. **A574**, 521 (1994).
[3] Amita *et al.*, At. Data Nucl. Data Tables **74**, 283 (2000); see www.nndc.bnl.gov/nndc/mag-dip-rot-bands, 2001.
[4] S. Frauendorf, Nucl. Phys. **A557**, 259c (1993).
[5] S. Frauendorf, Z. Phys. A **A358**, 163 (1997).
[6] R. M. Clark *et al.*, Phys. Rev. Lett. **78**, 1868 (1997).
[7] R. M. Clark *et al.*, Phys. Rev. Lett. **82**, 3220 (1999).
[8] H. Schnare *et al.*, Phys. Rev. Lett. **82**, 4408 (1999).
[9] S. Lakshmi *et al.*, Phys. Rev. C **66**, 041303(R) (2002).
[10] N. Xu *et al.*, Phys. Rev. C **39**, 1799 (1989).
[11] E. S. Paul *et al.*, Phys. Rev. C **40**, 1255 (1989).
[12] R. Ma *et al.*, Phys. Rev. C **41**, 2624 (1990).
[13] M. Muller-Veggian *et al.*, Nucl. Phys. **A417**, 189 (1984).

[14] A. Gade *et al.*, Nucl. Phys. **A673**, 45 (2000).
[15] N. J. O'Brien *et al.*, Phys. Rev. C **59**, 1334 (1999).
[16] P. K. Joshi *et al.*, Nucl. Instrum. Methods Phys. Res. A **399**, 51 (1997).
[17] M. Saha Sarkar *et al.*, Nucl. Instrum. Methods Phys. Res. A **491**, 113 (2002).
[18] K. Starosta *et al.*, Nucl. Instrum. Methods Phys. Res. A **423**, 16 (1999).
[19] N. R. Johnson *et al.*, Phys. Rev. C **55**, 652 (1997).
[20] L. C. Northcliffe *et al.*, Nucl. Data, Sect. A **7**, 233 (1970).
[21] V. I. Dimitrov *et al.*, Phys. Rev. C **62**, 024315 (2000).
[22] C. J. Pearson *et al.*, Phys. Rev. Lett. **79**, 605 (1997).